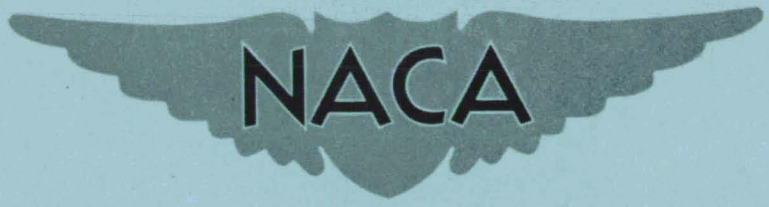

RESEARCH MEMORANDUM

EFFECTS OF AUXILIARY AND EJECTOR PUMPING ON THE MACH NUMBER ATTAINABLE IN A $4\frac{1}{2}$- BY $4\frac{1}{2}$-INCH SLOTTED TUNNEL AT LOW PRESSURE RATIOS

By John S. Dennard and Barney H. Little, Jr.

Langley Aeronautical Laboratory
Langley Field, Va.

NATIONAL ADVISORY COMMITTEE
FOR AERONAUTICS

WASHINGTON

January 22, 1954
Declassified August 16, 1957

NACA RM L53K19

NATIONAL ADVISORY COMMITTEE FOR AERONAUTICS

RESEARCH MEMORANDUM

EFFECTS OF AUXILIARY AND EJECTOR PUMPING ON THE MACH NUMBER ATTAINABLE IN A $4\frac{1}{2}$- BY $4\frac{1}{2}$- INCH SLOTTED TUNNEL AT LOW PRESSURE RATIOS

By John S. Dennard and Barney H. Little, Jr.

SUMMARY

An investigation has been made to determine the pressure ratios required to operate a slotted tunnel through a range of Mach number between approximately 0.6 to 1.4 where the speed variation is effected by (1) removal of air from the main stream by auxiliary pumping, (2) use of a main-stream-operated ejector located downstream of the test section, or (3) use of combinations of these methods. The tunnel used for these tests was of constant-area test section, $4\frac{1}{2}$ by $4\frac{1}{2}$ inches, with three diffuser-entrance cross sections which formed three configurations. In each configuration the amount of slot-flow air ejected was controlled by a flap in each slot of the tunnel floor.

For the case in which no auxiliary pumping was used, data were taken to find M_c, the Mach number attainable in the test section, for varying pressure ratios across the tunnel and varying positions of the slot-flow-control flaps for all three configurations. In two configurations, data were taken to find the test section Mach number as a function of bleed flow for a number of pressure ratios and flap positions. These data were taken at Reynolds numbers between 4×10^6 and 7×10^6 per foot.

It was found that for operation without bleed the main effect of the flaps was to fix the choking Mach number in the tunnel. For operation with bleed for the range of Mach number and bleed-flow ratio investigated, the incremental Mach number obtained with an incremental percentage of mass flow bled off was approximately a constant (0.1 increase in Mach number for 3.5-percent bleed flow) and was little affected by pressure ratio, flap position, and Mach number. For most economical operation the diffuser-entrance area should be chosen no larger than is necessary to obtain the maximum desired Mach number.

Application of these data to practical problems showed substantial power savings could be realized in a slotted tunnel by the use of auxiliary bleed.

INTRODUCTION

The recent development of the slotted throat has made transonic wind-tunnel operation not only possible but practical. As a result several large-scale transonic tunnels are in operation. Examples of these are the Langley 8-foot transonic tunnel (ref. 1) and the Langley 16-foot transonic tunnel (ref. 2). These tunnels, however, require considerably more power than do closed throat tunnels of comparable size. A comparison has been made in reference 1 to show that at a Mach number of 1.1 the power required for operation of a slotted test section is about 1.5 times as much as that for a solid test section. It is also shown in reference 1 that the power problem focuses on the region where the slot flow rejoins the main stream going into the diffuser. Not only are the local power losses large in that region, but also it is there that the performance of the diffuser is considerably affected since the inlet boundary-layer flow of the diffuser largely determines the efficiency of that component.

The tunnels described in references 1 and 2 both operate on the principle whereby the main stream from the test section is used as an ejector to pump air out of the slots. There is, however, another method of disposing of this slot flow involving the use of an auxiliary pump to remove all or a part of the slot flow from the plenum chamber around the test section and return it to the stream at some point downstream. It has been used extensively in small-scale slotted-tunnel installations - primarily to enable these facilities to operate at Mach numbers much higher than those which the drive compressors could provide. Examples of the use of this method for this purpose are given in references 3 and 4 although in these reports no particular attention was called to its use. It has never been determined whether the removal of bleed flow from the slot chamber by means of auxiliary pumps is better from the standpoint of total power consumed than the method of using the main stream as an ejector. An attempt has been made in reference 5 to compare analytically the known power requirements of a conventional slotted tunnel with some assumed power requirements for a bleed system, and the conclusion was reached that neither system was better than the other. In the analysis, however, the author assumed that the increase in diffuser efficiency resulting from the use of a bleed system was small. Actually, the power savings from such increased diffuser efficiency could be considerable because of the excellent velocity profile available at the diffuser entrance when using the auxiliary-pump bleed system. This is pointed out in reference 6 in which the power requirements of several slotted test sections were measured. In this reference also it was concluded that at Mach numbers less than 1.2 the use of an auxiliary pump for slot-flow removal provided power parameters less than those for any ejector configuration tested.

The purpose of this investigation is to determine the relative advantages of the two systems of handling slot flow and to measure the effect of combining varying amounts of bleed flow with ejector pumping by the main stream. This is done by measuring the Mach number attainable in a model tunnel at a constant pressure ratio but with varying rates of bleed flow and with different slot-flow reentry conditions.

A $4\frac{1}{2}$- by $4\frac{1}{2}$-inch test section with 4 slots in the top and bottom floors followed by a diffuser having a 2:1 area ratio was used in this investigation. Slot-flow reentry flaps were placed between the floor bars at the downstream end of the slots. The flap trailing edge was hinged at the diffuser inlet and the hinge-line position was variable. All data were obtained at Reynolds numbers from 4×10^6 to 7×10^6 per foot.

SYMBOLS

H_o	reference total pressure
H_d	computed diffuser-exit total pressure
p	local static pressure
p_a	atmospheric pressure
p_c	static pressure in test section
M_c	Mach number computed from p_c and H_o
M_d	computed diffuser-exit Mach number
m	mass flow through nozzle
m'	mass flow bled out of test section
δ_F	flap angle from closed position
h	tunnel height, 4.5 in.
y	distance of diffuser floor surface outboard of slotted floor surface
hp	horsepower

APPARATUS AND METHOD

A $4\frac{1}{2}$- by $4\frac{1}{2}$-inch test section with slotted floors on the top and bottom walls followed by a two-dimensional diffuser having a 2:1 area ratio and diverging top and bottom walls was the subject of this investigation. The nozzle alone is shown in figure 1(a) and the nozzle and diffuser are shown in figure 1(b).

Tunnel.- The slotted floors which can be seen in figures 1(a) and 1(b) are slightly modified versions of the variable-depth, long-taper slotted floors described in reference 3. In that reference it is shown that these floors give good center-line Mach number distributions up to a Mach number of about 1.4. The modifications were:

(1) The stem depth of the floor bars was increased by $1\frac{1}{4}$ inches to channel the slot flow more completely

(2) The floor bars were tapered or boattailed at the downstream end

(3) Slot-flow guide flaps were added in the slot channels between the bars

The flaps were 1 tunnel height in length and 1/8 inch thick, and the leading and trailing edges were rounded to a 1/16-inch radius. They were hinged at the trailing edge in such a way that the upper surface of the flap alined with the diffuser wall. The leading-edge position could be set at any point between the top and bottom of the floor bars. The clearance between the flaps and the floor bars was kept at a minimum. The position of the flaps δ_F was measured from the position where the leading edge was up against the floor surface (see fig. 2). The flap position was remotely controlled by a lever and gear system.

In figure 1, configuration II is shown, in which the ratio of the distance from the floor surface to the flap hinge line y to the half-tunnel height $h/2$ is 0.239. In configuration I, $\frac{y}{h/2} = 0.106$ and in configuration III, $\frac{y}{h/2} = 0.461$. For each configuration a separate set of diffuser blocks was made and, although the diffuser-inlet height changed, the exit height and the length were held constant. The contours of the three configurations are shown in figure 2. It should be noted that at any given flap angle the position of the leading edge of the flaps relative to the floor surface is independent of hinge-line position.

Flow system.- A line diagram of the tunnel flow system is shown in figure 3. The nozzle was enclosed in a cylindrical plenum chamber

30 inches in diameter. This chamber was sealed except where the bleed-flow connection was made. The main air flow through the nozzle was supplied by a compressor capable of delivering a maximum pressure of 2 atmospheres. Air was bled from the test-section chamber by means of a vacuum pump completely independent of the main drive. The amount of air bled from the chamber was controlled by a butterfly valve in the line from model to pump and a bypass valve on the intake of the pump and metered by means of a calibrated sharp-edge orifice in the bleed line. At the diffuser exit air was dumped into a 30-inch duct which exhausted to the atmosphere.

Instrumentation.- Static-pressure orifices were installed at a station in the inlet of the nozzle, in the plenum chamber, and in the model side wall from the flap hinge line down through the diffuser. The location of these side-wall tubes is shown in figure 2. Reference total pressures and temperatures were read in the 30-inch-diameter duct upstream of the nozzle and sufficient pressure taps were installed in the bleed line to measure the flow there. All pressures were measured on a multitube mercury manometer board, and photographs of this board were taken at each point during the runs. The auxiliary bleed-flow-measuring orifice plate was calibrated by using a venturi of known flow coefficient. Care was taken to ascertain that there was no leakage in the bleed-flow system.

Test procedure.- The zero-bleed data were taken with the bleed line blanked off by replacing the orifice with a solid plate. The flap angle was set and the Mach number M_c was measured as the total pressure was varied by varying the speed of the main-drive compressor. This process was repeated for each flap angle.

In the variable-bleed investigation the orifice plate was installed in the vacuum line, the flap angle was set, the total pressure was set by holding the main-drive-compressor speed constant, and the Mach number M_c was measured as the valves in the bleed line were adjusted to give different bleed-flow ratios. This process was repeated over a range of total pressure and flap angle.

Data reduction.- The test-section Mach number M_c was computed from the test-section plenum-chamber static pressure p_c and the reference total pressure H_o. The bleed mass flow m' was computed from the pressure ratio across the calibrated orifice plate. The main-stream mass flow was computed from the test-section inlet static pressure assuming a flow coefficient of 1.00.

The ratio of reference total pressure to atmospheric pressure H_o/p_a was used as a parameter indicative of power required. Since the flow at the diffuser exit was always subsonic, the atmospheric pressure was assumed to be equal to static pressure at the diffuser exit station.

RESULTS AND DISCUSSION

Operation Without Bleed Flow

Effect of pressure ratio.- The pressure ratios H_o/p_a required to generate various Mach numbers for $\delta_F = 0^\circ$, 10°, and 20° for each of the three gap ratios are presented in figure 4. For configuration I $\frac{y}{h/2} = 0.106$ (fig. 4(a)) at $\delta_F = 0^\circ$ the Mach number rises rapidly with pressure ratio up to about $M_c = 0.95$ for $H_o/p_a = 1.3$. At higher pressure ratios the Mach number changes only slightly and the tunnel never attained sonic velocities since the 0° flap angle precludes the effective removal of slot-flow air from the plenum; consequently, the tunnel chokes in the region near the leading edge of the flaps which is, at this flap angle, effectively a second minimum. Increasing the flap angle to 10° or 20° produces little or no change in the Mach number at low values of H_o/p_a. Increasing the pressure ratio at these higher flap angles causes the Mach number to rise rapidly to about 1.1 where it again levels off because of choking near the station of the flap hinge line. Slightly higher Mach numbers were reached at $\delta_F = 10^\circ$ than at 20° since, at $\delta_F = 20^\circ$, low-energy flow and poor flow conditions exist at the leading edge of the flap. Also, at $\delta_F = 20^\circ$, the high deflection angle causes flow separation at the flap hinge line and a small effective second minimum is formed with attendant choking and Mach number limitations.

For the medium gap ratio, configuration II $\frac{y}{h/2} = 0.239$ (fig. 4(b)), the curves show a similar rise in Mach number with increasing pressure ratio but without the choking limitations at high flap angles observed for configuration I. Tests at $\delta_F = 0^\circ$ were not extended to high values of H_o/p_a, but the limited data obtained indicate a probable maximum Mach number very near the same value found for configuration I. At $\delta_F = 10^\circ$ and 20°, the Mach number rises with pressure ratio at about the same rate as observed for configuration I up to $H_o/p_a = 1.35$. Above this value, at which configuration I choked, the rate of Mach number increase is reduced and the tunnel appears to be approaching a choked condition near the upper limit of the test range ($H_o/p_a = 1.9$ and $M_c = 1.32$).

At $\frac{y}{h/2} = 0.461$, configuration III (fig. 4(c)), the data at $\delta_F = 0^\circ$ again exhibit a rise in Mach number with pressure ratio up to $H_o/p_a = 1.4$. At pressure ratios above 1.4, the tunnel chokes at a subsonic Mach number, and the choke persists to $H_o/p_a = 1.6$ where the Mach number increases

abruptly from 0.96 to 1.10. This abrupt jump occurs in a range of Mach number and pressure ratio which is of little operational interest since it represents a condition requiring high power consumption for a relatively low Mach number. The mechanism of the jump phenomenon is of interest, however, and is associated with leakage of air through the small clearance allowed between the edges of the flap and the lower portion of the floor bars. For this large gap ratio, $\frac{y}{h/2} = 0.461$, the zero flap position presents a highly divergent passage over the flap and between the floor bars. At low pressure ratios, the stream does not flow in this highly divergent passage but, in effect, separates from the leading edge of the flap, leaving a region of reverse flow with low energy over the flap surface in each separate slot. As the pressure ratio is increased, the main tunnel air becomes and remains attached over the flap leading edge, producing very low pressures and high Mach numbers over the surface of the flap. The flow pattern changes abruptly and the low pressures, thus produced, induce a leakage flow from the plenum through the small flap clearances and into the diffuser. Based on relationships between a one-dimensional area ratio and the Mach number, the leakage flow necessary to produce this abrupt increase in Mach number would be less than 1 percent of the total tunnel air flow. If the pressure ratio had been raised to a sufficient level, it is quite possible that a similar abrupt Mach number increase would have occurred with the gap ratio of 0.239. It is noted that the initial rise in Mach number with pressure ratio is somewhat less rapid for configurations II and III than for configuration I at the 0° flap position. It is believed that this difference is due to losses produced by the sudden enlargement in cross section at the entrance to the mixing tube and to subsequent losses in diffuser performance.

Increasing δ_F to 10° or 20°, figure 4(c), again makes very little change in the Mach number generated at low values of H_o/p_a. With increasing pressure ratio, the Mach number increases at about the same rate as for configuration II (fig. 4(b)) up to $H_o/p_a = 1.65$. Above this point the Mach number continues to rise smoothly for $\delta_F = 20^\circ$, and a small abrupt jump occurs for $\delta_F = 10^\circ$. This jump is attributable to leakage, as in the case for $\delta_F = 0^\circ$, which is induced by low-pressure air over the surface of the flap. This low-pressure region is again the result of an expansion from the leading edge of the flap under the influence of a high pressure ratio. The jump is followed by a choked region of constant Mach number.

Diffuser static-pressure distributions.- In figures 5, 6, and 7 are presented several typical diffuser static-pressure distributions for $\delta_F = 0^\circ$ and 10° for each of the three gap ratios. For $\frac{y}{h/2} = 0.106$ at $\delta_F = 0^\circ$, figure 5(a), the diffuser presents a typical subsonic pressure rise at the lower pressure ratios. For these low pressure ratios, the

static pressure in the constant-cross-section mixing tube is very nearly constant, rising only slightly under the influence of the diffusion afforded by the sudden increase in area from the downstream end of the floor bars to the mixing tube. Increasing the pressure ratio above 1.35 causes no further changes in the static-pressure distribution in the mixing section but provides a stable pattern of relatively weak shocks and expansions. Above $H_o/p_a = 1.35$, however, a Prandtl-Meyer turn occurs at the diffuser entrance with, at the higher pressure ratios, rapid expansion to high supersonic Mach numbers. The supersonic acceleration is then followed by a normal shock and subsonic diffusion to the exit of the diffuser. It is, of course, obvious that operation with supersonic flow in the diffuser is wasteful of power and should be avoided whenever possible. For $\delta_F = 10^\circ$, figure 5(b), a similar set of data is obtained where the mixing-tube static-pressure distribution remains unchanged at all pressure ratios above about 1.35 and the diffuser entrance produces Prandtl-Meyer turns to low pressures and high supersonic velocities. Reference to figure 4(a) shows that everywhere the mixing-tube static-pressure distribution becomes fixed corresponds to a choked condition in the tunnel test section and all further increases in pressure ratio (and power) are only dissipated in increasingly stronger normal shocks in the diffuser.

For configuration II $\frac{y}{h/2} = 0.239$ at $\delta_F = 0^\circ$ only a limited pressure-ratio range was investigated and a choked condition was never attained (fig. 6(a)); the static-pressure distributions generally following the typical subsonic pattern. For $\delta_F = 10^\circ$, figure 6(b), at the highest pressure ratio $H_o/p_a = 1.821$, the distribution in the mixing tube indicates the existence of both shocks and expansions but no expansion originated at the diffuser entrance. This point appears to be the beginning of choke for this configuration and further increases in pressure ratio would only be wasteful of power.

Static-pressure distributions for configuration III $\frac{y}{h/2} = 0.461$ at $\delta_F = 0^\circ$ are presented in figure 7(a). Here, at low pressure ratios, an appreciable amount of subsonic diffusion is accomplished in the mixing tube under the influence of the abrupt expansion from the downstream end of the slotted floors to the mixing tube. A slight increase in pressure ratio from 1.58 to 1.61 produces the widely differing patterns of static pressure noted in the figure. This change in pattern corresponds to the abrupt jump in Mach number noted in figure 4(c). It is interesting to note that the Mach lines corresponding to the Mach numbers indicated by the pressures between stations -5 and -1.5 can be projected forward to the leading edge of the flaps. These static-pressure distributions, then, offer confirmation of the expansion over the leading edge of the flap and subsequent leakage which is responsible for the sudden increase in Mach number shown in figure 4(c).

Increasing the flap angle to 10° produces the distributions shown in figure 7(b). Here at low pressure ratios the pattern is again typical of the subsonic diffuser. As the pressure ratio increases to 1.45 and 1.65, the distribution through the mixing region flattens and, at $H_o/p_a = 1.71$, an expansion occurs through the mixing-tube region, the origin of which can again be traced to the vicinity of the leading edge of the flap. These conditions are again indicative of high power consumption with strong shocks occurring at excessively high Mach numbers in the diffuser.

Observations from zero-bleed data.- From these data it can be deduced that, for zero-bleed-flow conditions, the flow changes effected by flap deflection result primarily from the flap characteristic of fixing the choking Mach number in the tunnel. For $\delta_F = 0°$, choking always occurred near the leading edge of the flap. At $\delta_F = 10°$ and 20°, configurations I and II choked at the flap hinge line, producing a series of relatively weak shocks and expansions in the mixing tube. The largest gap ratio $\frac{y}{h/2} = 0.461$, configuration III, choked at the flap leading edge for $\delta_F = 10°$ as evidenced by the sudden change in static-pressure distribution and the Prandtl-Meyer turn for all pressure ratios above 1.71. If operation is attempted at high pressure ratios and low flap angles for a large gap ratio in a geometrically similar test section, leakage flow may occur and cause abrupt changes in the test-section Mach number. It is important, however, to select a gap large enough to generate the desired Mach number without choking.

Operation With Auxiliary Bleed Flow

Two of the test configurations $\frac{y}{h/2} = 0.239$ and 0.461 have been tested using an auxiliary bleed air pump to supplement the flaps in handling the bleed air flow. Results of these tests are presented in figure 8.

Effect of varying bleed flow.- The variation of Mach number with auxiliary bleed flow rate for three different flap angles for configuration II is presented in figure 8(a). Each curve represents a constant value of pressure ratio and all curves are nearly straight with approximately a uniform slope, $\frac{\Delta M_c}{\Delta \frac{m'}{m}} = \frac{0.1}{0.035}$; this result indicates that the bleed-flow quantity required for a specified change in Mach number is independent of flap angle, gap ratio, pressure ratio, and Mach number. It is interesting to note that this slope is near that predicted by the theoretical relationship between a one-dimensional area ratio and the Mach number for the range between $M = 1.1$ and $M = 1.4$, $\frac{\Delta M_c}{\Delta \frac{m'}{m}} = \frac{0.1}{0.0314}$.

In the range near $M_c = 1.0$ the slope of these curves changes slightly, more noticeably for the lower flap angles. This is largely attributed to the fact that, for the theoretical relationship between a one-dimensional area ratio and the Mach number, a small increase in area causes rapid changes in Mach number in the range near $M = 1.0$.

For all Mach numbers less than 1.0, it is noted that the positive slope of these curves is contrary to that expected on the basis of the theoretical relationship between a one-dimensional area ratio and the Mach number. The fact that both the subsonic and supersonic ranges have the same slope appears to be fortuitous. For the low subsonic Mach numbers, the withdrawal of bleed air so improves the boundary layer and diffuser performance that larger quantities of air are handled by the tunnel and the Mach number is thus increased. At high subsonic Mach numbers where choking occurs in the region near the flaps, auxiliary bleed air obviously can alleviate choking and cause increases in tunnel Mach number.

The dashed line shown in figure 8(a) is taken from reference 6 and is indicative of the required bleed flow in a tunnel of constant cross section at a constant value of H_o/p_a where it is intended that none of the slot flow should be returned to the main stream. This curve which approximately parallels the present data again illustrates the near linearity of ΔM_c with $\Delta\frac{m'}{m}$ through most of the Mach number range and also illustrates the increase in slope near $M_c = 1.0$. The data for configuration III, shown in figure 8(b), again exhibit a nearly uniform slope of $\frac{\Delta M}{\Delta\frac{m'}{m}} = \frac{0.1}{0.035}$ for constant values of H_o/p_a at the four flap angles tested. The changes in slope of these curves near $M_c = 1.0$ is less pronounced than for the curves of configuration II because of low-pressure-induced leakage flow around the edges of the flaps. With increasing flap angles, the curves again remain essentially straight and parallel as was the case for configuration II.

Effect of flap angle.- The data of figures 4 and 8 have been cross-plotted in figure 9 to show the bleed flow required at various flap angles and a constant pressure ratio to obtain a specified Mach number. For configuration II, figure 9(a), these curves indicate a very slight variation of m'/m with flap angle up to $\delta_F = 10^\circ$. Above $\delta_F = 10^\circ$, the lower values of H_o/p_a require increasing amounts of m'/m with increasing δ_F, whereas for the higher values of H_o/p_a, 1.35 at $M_c = 1.3$, the opposite is true. It appears that at low values of H_o/p_a, the shock occurs forward of the flap hinge line and the high-pressure air behind the shock wave tends to run into the plenum; thus an increase in flap angle reduces the restriction to the reverse flow and thereby increases

the bleed-flow requirements. At high values of H_o/p_a, the shock is in the mixing tube and the high-pressure air behind the shock cannot move into the plenum; opening the flaps, therefore, increases the induction pumping by the main stream and reduces the bleed-flow requirements. It is interesting to note that a value of H_o/p_a near 1.2 would offer a nearly constant bleed-flow requirement for a given Mach number regardless of flap angle.

Increasing the gap ratio to $\frac{y}{h/2} = 0.461$, configuration III, gives the results shown in figure 9(b). Here, for the lower values of Mach number and H_o/p_a, it appears that a flap angle of about 5° would be optimum in regard to bleed-flow requirements. Above $\delta_F = 5^\circ$ there is, as in configuration II, a tendency for m'/m to increase with increases in δ_F; this tendency again is stabilized or even reversed at the higher values of H_o/p_a. For this gap ratio there is no single value of H_o/p_a which will provide a constant bleed-flow requirement at all flap angles, but rather several values are noted between $H_o/p_a = 1.18$ and 1.3 depending on the Mach number.

A comparison of configurations II and III shows that for given values of H_o/p_a, δ_F, and M_c, the smaller gap ratio will almost always require less auxiliary bleed flow. Operation with either gap ratio is possible at minimum bleed-flow requirements at flap angles of 10° except at the higher Mach numbers and pressure ratios. For higher values of M_c or H_o/p_a, a larger flap angle is desirable.

Estimates of Power Requirements

On the basis of data for configuration II $\frac{y}{h/2} = 0.239$ and the assumption that H_o/p_a remains fixed, it is concluded that a tunnel which could be operated up to $M_c = 1.0$ at $\delta_F = 10^\circ$ without auxiliary pumping could operate at $M_c = 1.1$ using $1\frac{1}{2}$-percent auxiliary bleed air and at $M_c = 1.2$ using $4\frac{1}{2}$-percent auxiliary bleed air. (See fig. 8(a).) These bleed flow rates have been applied to a power-requirement example with the following considerations:

In order to make the example applicable to most wind tunnels in operation it is assumed that the inlet total pressure H_o remains constant. An idealized flat diffuser-exit velocity profile determined by the measured static pressure and the known mass flow was assumed. With these assumptions and the values of M_c, H_o/p_a, and m'/m just given, the following table can be calculated:

M_c	$\frac{m'}{m_o}$	$\frac{H_o}{p_a}$	M_d	$\frac{H_o}{H_d}$	$\frac{hp_{total}}{hp_{no\ bleed}}$	$\frac{hp_{total}}{hp_{M=1.0}}$	$\frac{hp_{main}}{hp_{M=1.0}}$	$\frac{hp_{aux}}{hp_{M=1.0}}$
1.0	0	1.25	0.356	1.145	-----			
1.1	0	1.32	.376	1.198	-----	1.342	1.342	
1.1	.015	1.25	.352	1.147	0.808	1.084	1.010	0.0739
1.2	0	1.45	.412	1.290	-----	1.910	1.910	
1.2	.045	1.25	.341	1.153	.694	1.323	1.054	.269

The hp ratios in the table are based on isentropic compression, and the main-drive power and bleed-air power are weighted on a mass-flow basis to arrive at the total required power. The bleed-air power is that necessary to compress the bleed air from the plenum static pressure to the diffuser-exit total pressure. This example is, perhaps, not exact in its power ratios but does illustrate the approximate savings in power that may be realized by the use of auxiliary bleed air pumps to supplement the main tunnel drive in generating Mach numbers in the range of these tests. It is noted that, at constant values of H_o/p_a, the auxiliary hp increases rapidly with M_c, but there is still a considerable saving in total power over that required to operate at the higher Mach numbers with no auxiliary bleed flow.

A comparison of the power required for varying amounts of auxiliary bleed flow at a constant Mach number is shown in the following example. The Mach number is chosen as 1.2; in addition, $\frac{y}{h/2} = 0.239$ and $\delta_F = 10^\circ$.

$\frac{m'}{m}$	$\frac{H_o}{p_a}$	M_d	$\frac{H_o}{H_d}$	$\frac{hp_{total}}{hp_{no\ bleed}}$	$\frac{hp_{main}}{hp_{no\ bleed}}$	$\frac{hp_{aux}}{hp_{no\ bleed}}$	$\frac{hp_{aux}}{hp_{main}}$
0	1.45	0.412	1.290				
.02	1.35	.377	1.224	0.845	0.788	0.0572	0.0728
.08	1.18	.311	1.104	.649	.381	.269	.705

The ratio of auxiliary power to main-tunnel power increases rapidly with m'/m, but the total power is reduced to approximately 65 percent

of the zero-bleed value by increasing the bleed to 8 percent. At this operating condition, the bleed-pump power will be 70 percent of the main-tunnel power.

From these examples the conclusion may be drawn that, for a practical closed-circuit wind tunnel, the Mach number may be raised from 1.0 to 1.2 by the addition of an auxiliary bleed air pump to handle $4\frac{1}{2}$ percent of the total air flow at a pressure ratio of 2.1. The total power of the system would be 1.32 times the power to operate at Mach number 1.0 as compared to 1.9 if the system were operated using main-tunnel power only, and without an auxiliary pump. At a constant tunnel Mach number of 1.2, the auxiliary-pump power increases with bleed flow rate, but the main-stream power and total power decrease with increases in bleed flow rate. Diffuser-exit velocity profiles other than the idealized flat distribution may lead to power ratios slightly different from those of the preceding example.

CONCLUSIONS

On the basis of the data presented for this square-cross-section slotted tunnel, together with the practical examples of application of these data, the following conclusions have been formulated:

1. For operation of a slotted tunnel without auxiliary bleed air pumping, the Mach number changes effected by varying the flap deflection are caused primarily by changes in the effective minimum area and resultant choking near the test-section exit.

2. For operation in a configuration similar to this one at large gap ratios and low flap angles with unsealed flaps, leakage flow past the flaps may effect abrupt changes in Mach number as the pressure ratio is increased.

3. For operation with bleed for the range of Mach number and bleed-flow ratio investigated, the incremental Mach number obtained with an incremental percentage of mass flow bled off was approximately constant (0.1 increase in Mach number for 3.5-percent bleed flow).

4. For most economical operation, the gap ratio should be chosen no larger than is necessary to provide the maximum desired Mach number.

5. For 10° flap deflection and a gap ratio of 0.239, the test-section Mach number of this tunnel was increased from 1.0 to 1.1 by the use of auxiliary air pumps handling $1\frac{1}{2}$ percent of the total flow

and to 1.2 by the use of $4\frac{1}{2}$-percent bleed flow air. Calculations indicate that a $8\frac{1}{2}$-percent increase in over-all power would be required to increase the Mach number from 1.0 to 1.1 and 32-percent power increase is necessary to reach Mach number 1.2. If these Mach number increases were effected without the use of auxiliary pumping, main-stream power increases of the order of 34 and 91 percent would be required.

Langley Aeronautical Laboratory,
National Advisory Committee for Aeronautics,
Langley Field, Va., November 10, 1953.

REFERENCES

1. Whitcomb, Richard T., Carmel, Melvin M., and Morgan, Francis G., Jr.: An Investigation of the Stream-Tube Power Losses and an Improvement of the Diffuser-Entrance Nose in the Langley 8-Foot Transonic Tunnel. NACA RM L52E20, 1952.

2. Ward, Vernon G., Whitcomb, Charles R., and Pearson, Merwin D.: Air-Flow and Power Characteristics of the Langley 16-Foot Transonic Tunnel With Slotted Test Section. NACA RM L52E01, 1952.

3. Nelson, William J., and Cubbage, James M., Jr.: Effects of Slot Size and Geometry on the Flow in Rectangular Tunnels at Mach Numbers up to 1.4. NACA RM L53B16, 1953.

4. Nelson, William J., and Bloetscher, Frederick: Preliminary Investigation of a Variable Mach Number Two-Dimensional Supersonic Tunnel of Fixed Geometry. NACA RM L9D29a, 1949.

5. Osborne, James I.: Distribution of Losses in Model Transonic Wind Tunnel at a Mach No. of 1.25. Doc. No. D-11934, Boeing Airplane Co., June 19, 1951.

6. Dennard, John S.: A Preliminary Investigation of the Power Requirements of Slotted Test Section. NACA RM L53F10, 1953.

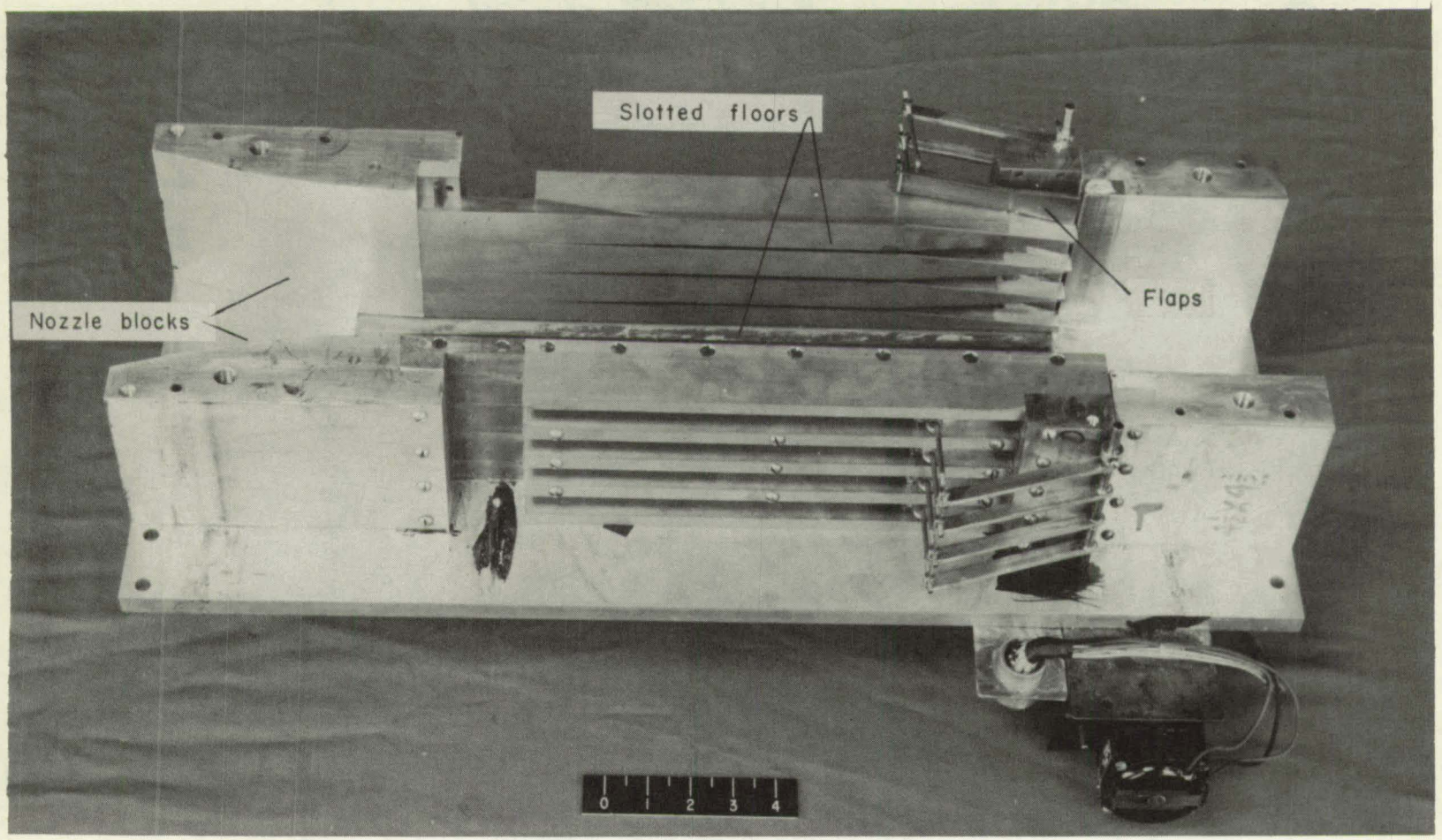

L-76862.1

(a) Test section assembly.

Figure 1.- Experimental model.

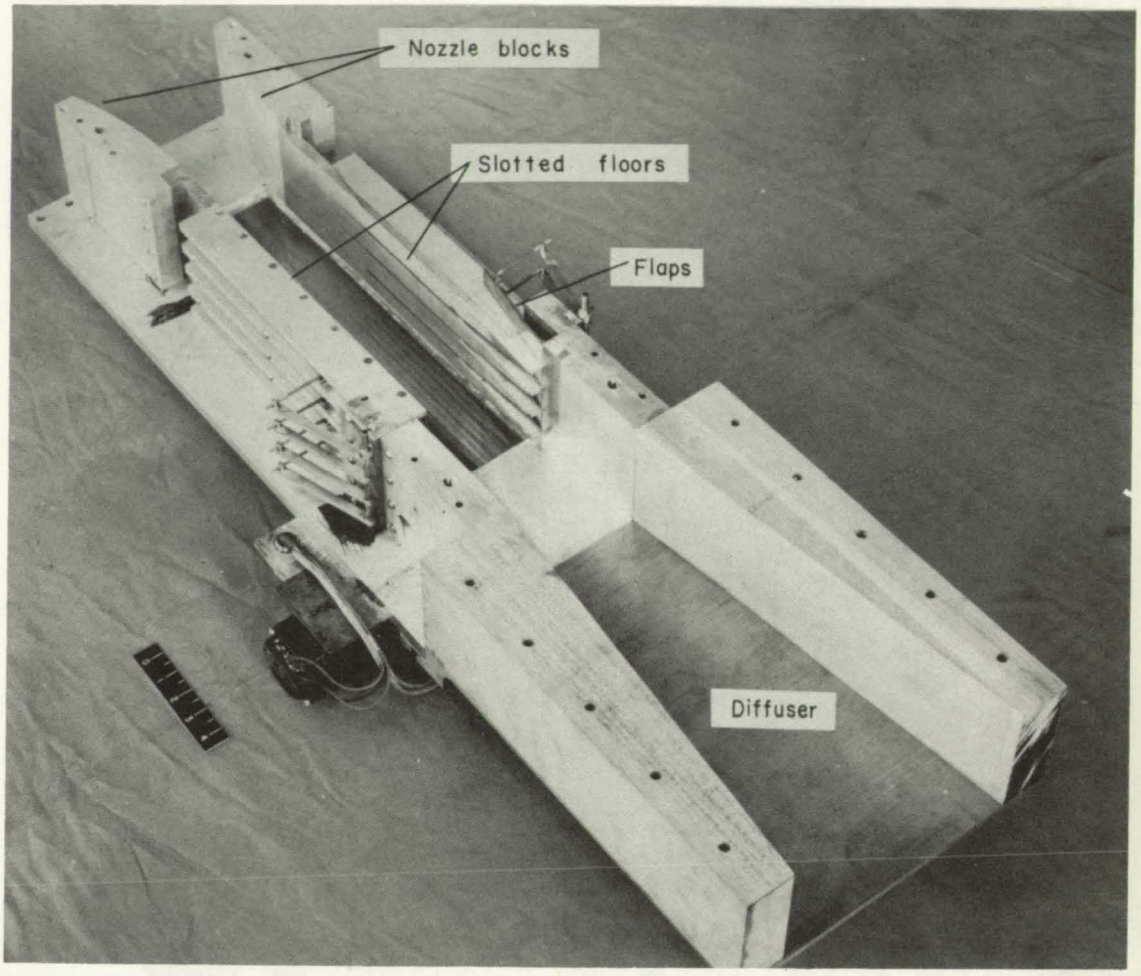

L-76861.1

(b) Test section and diffuser assembly.

Figure 1.- Concluded.

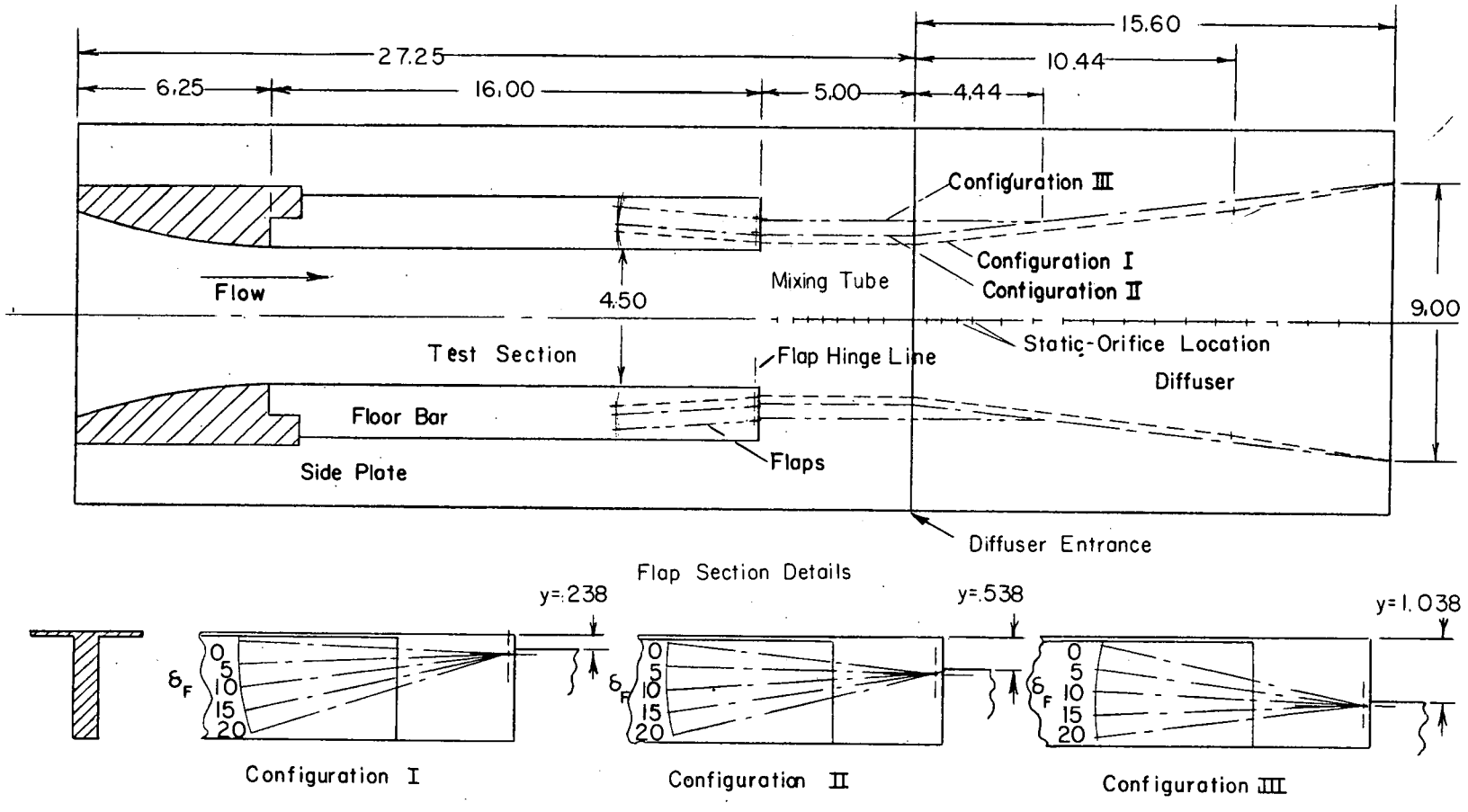

Figure 2.— Line diagram of nozzle and diffuser.

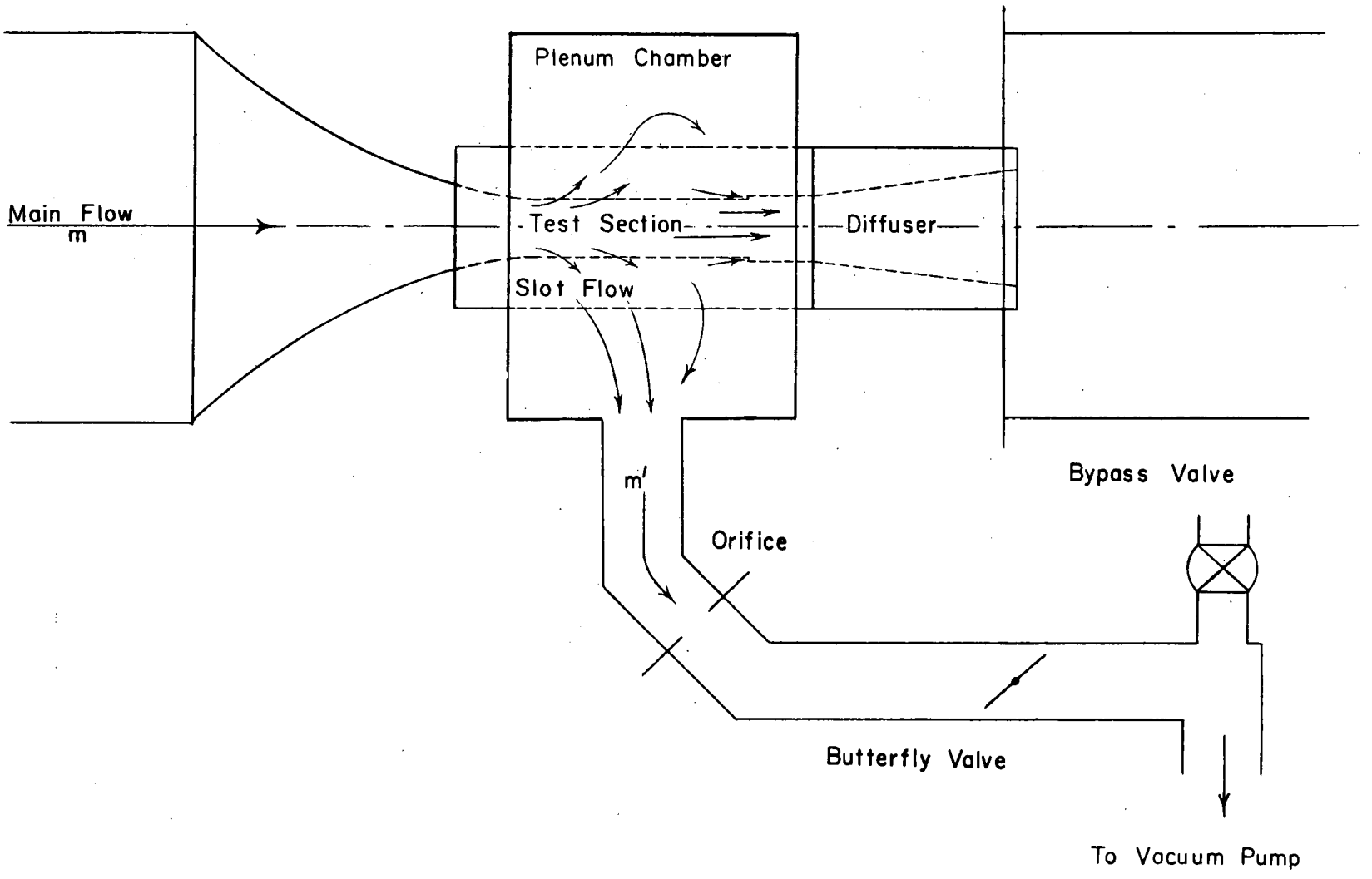

Figure 3.— Line diagram of model flow system.

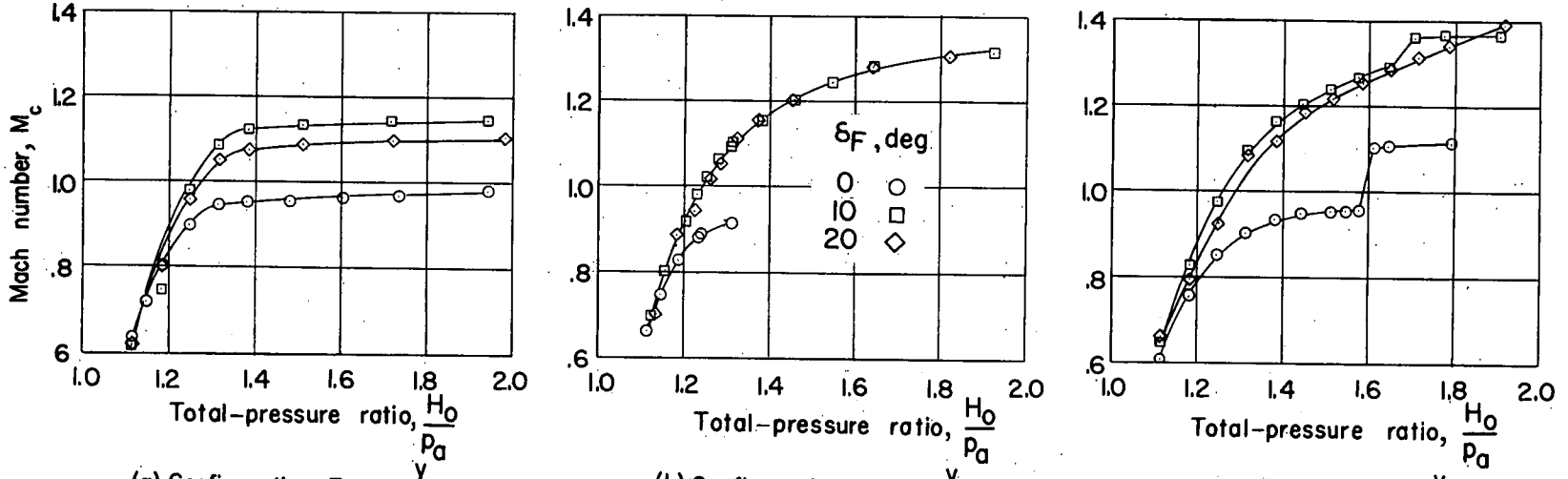

(a) Configuration I — $\frac{y}{h/2}$=.106. (b) Configuration II — $\frac{y}{h/2}$=.239. (c) Configuration III — $\frac{y}{h/2}$=.461.

Figure 4.— Variation of test-section Mach number with pressure ratio for the zero-bleed condition.

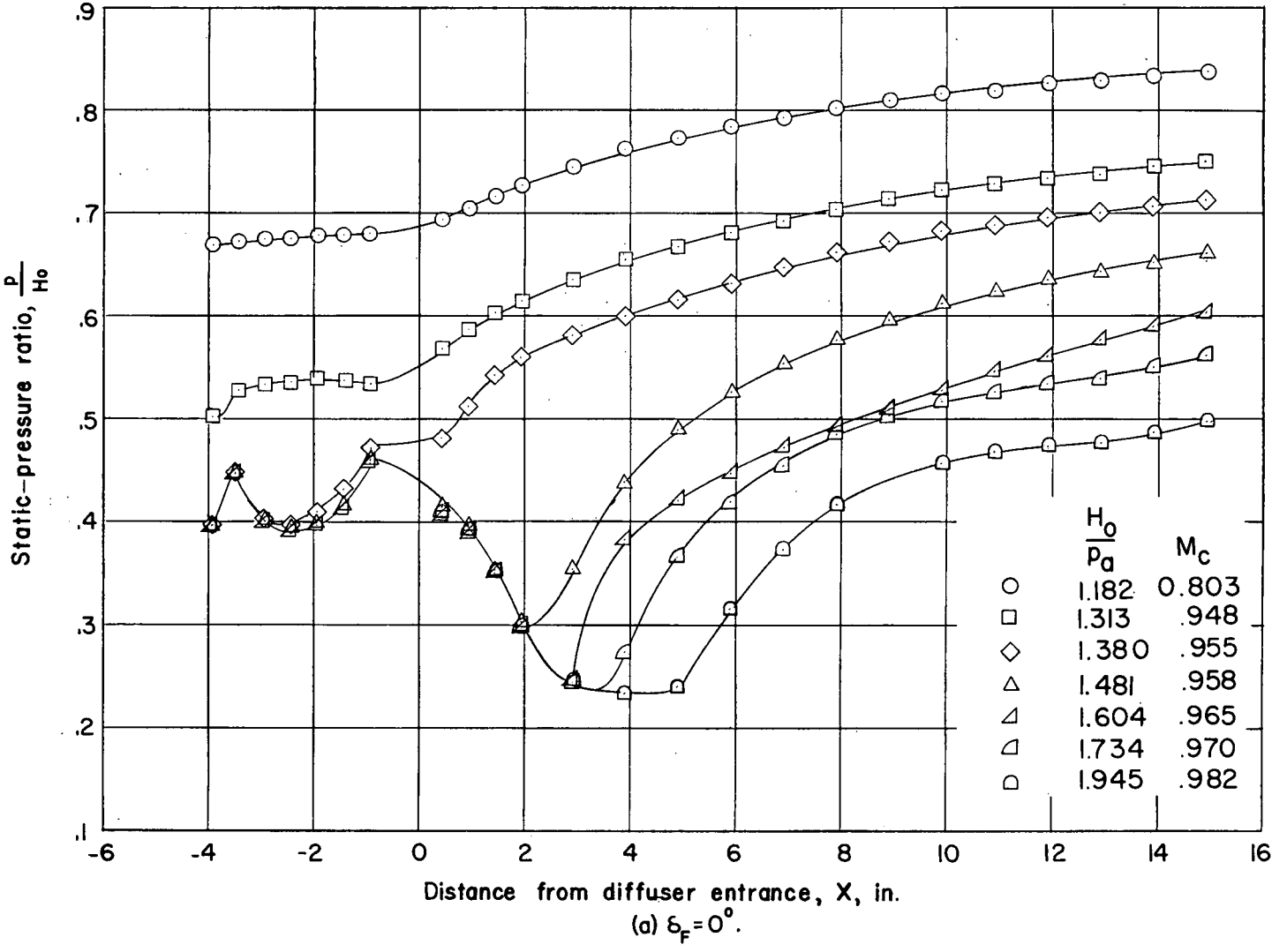

(a) $\delta_F = 0°$.

Figure 5.—Diffuser static-pressure distributions for zero-bleed condition. Configuration I $\frac{y}{h/2} = .106$.

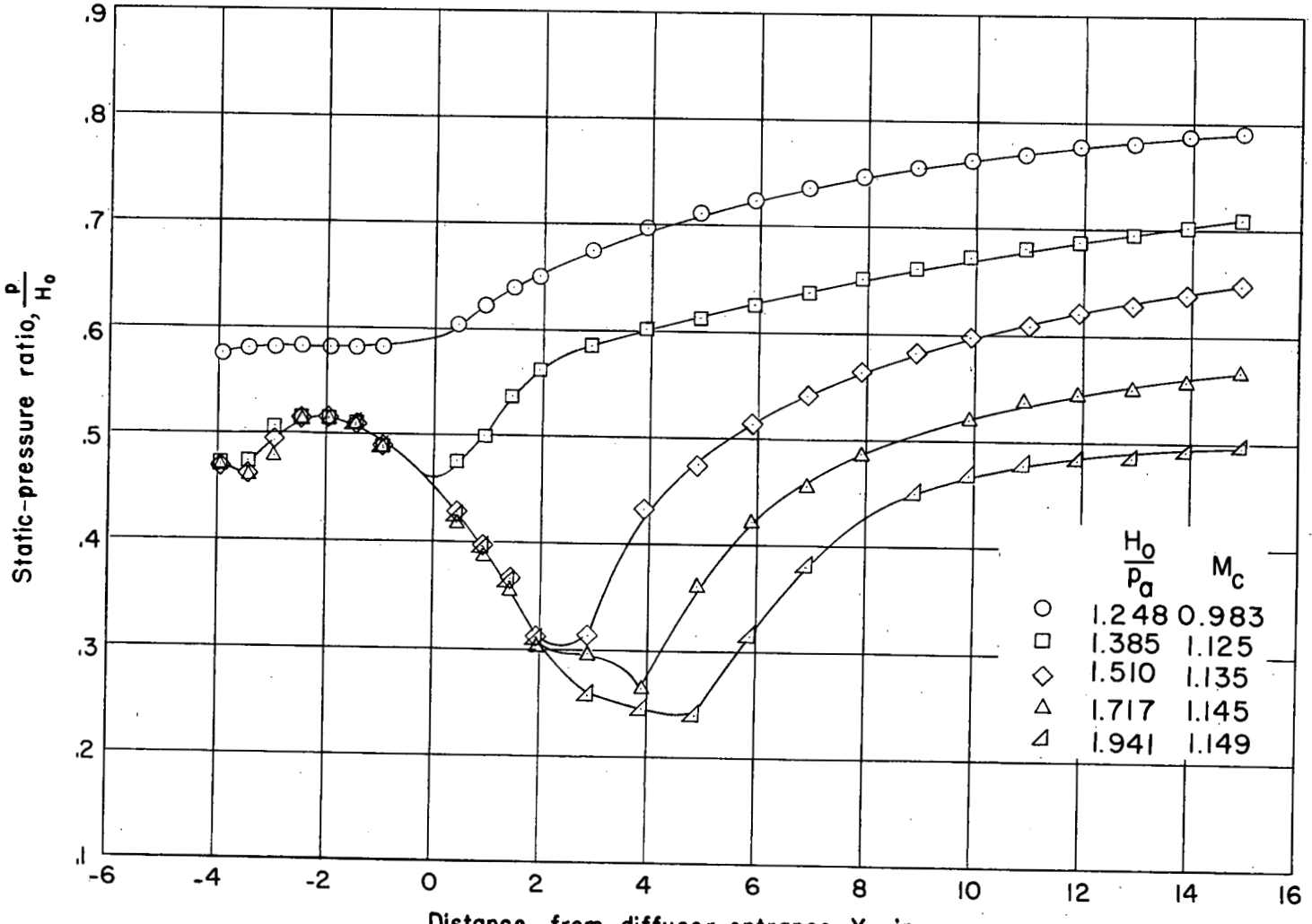

(b) $\delta_F = 10°$.

Figure 5.- Concluded.

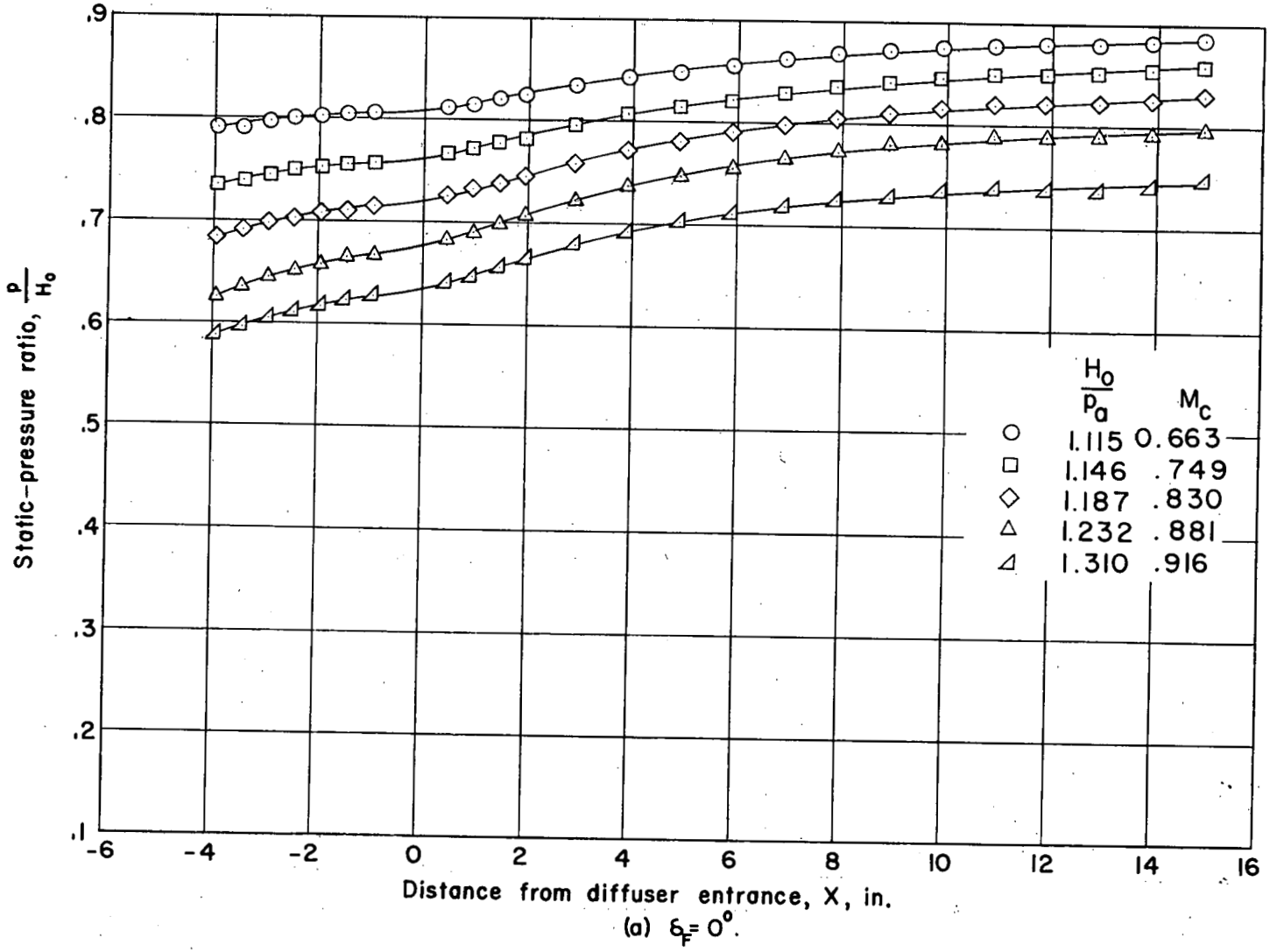

(a) $\delta_F = 0°$.

Figure 6.-Diffuser static-pressure distributions for zero-bleed condition. Configuration II $\frac{y}{h/2} = .239$.

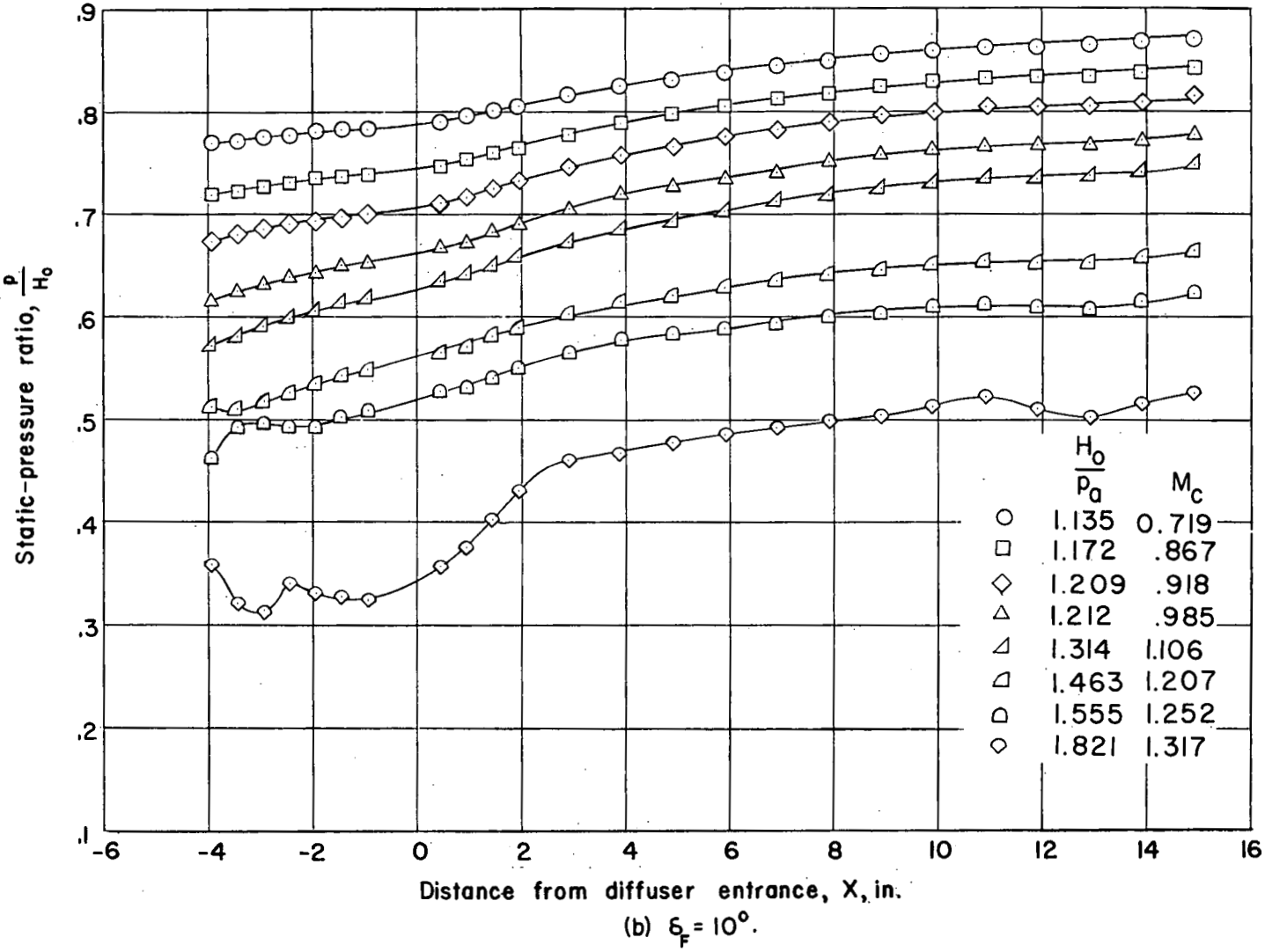

(b) $\delta_F = 10°$.

Figure 6 .— Concluded.

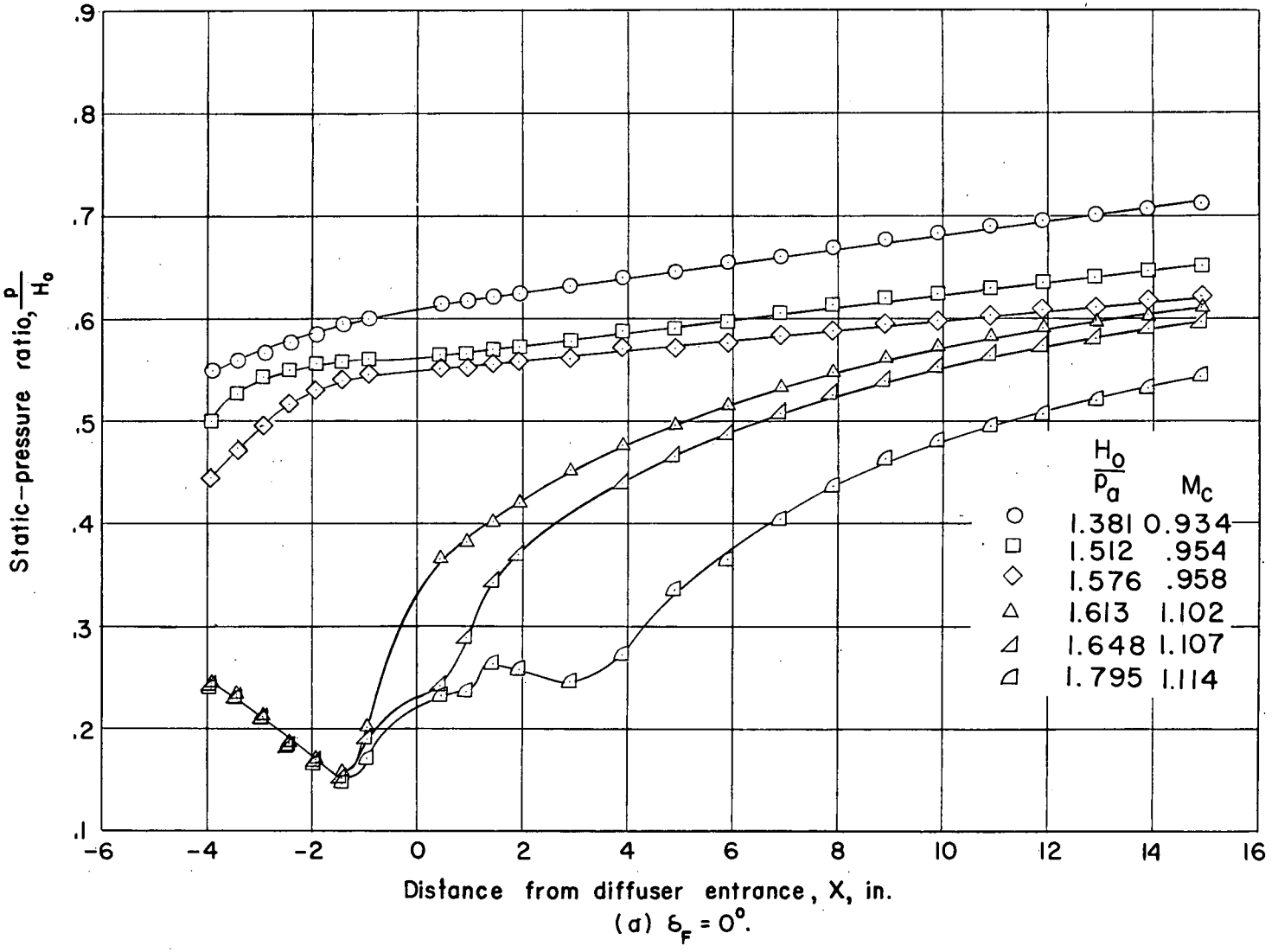

(a) $\delta_F = 0°$.

Figure 7.-Diffuser static-pressure distributions for zero-bleed condition. Configuration III $\frac{y}{h/2} = .461$.

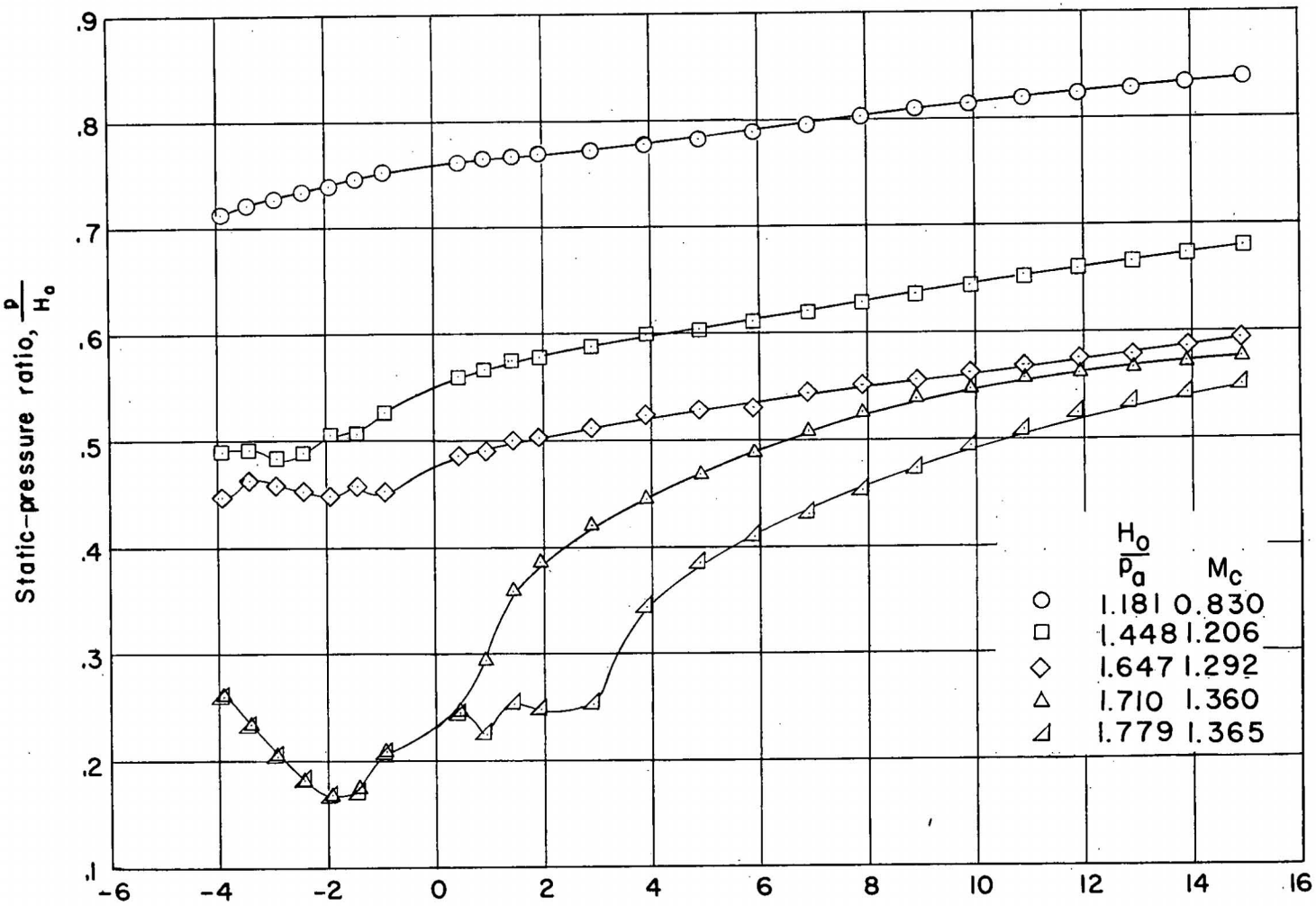

(b) $\delta_F = 10°$.

Figure 7 .-Concluded.

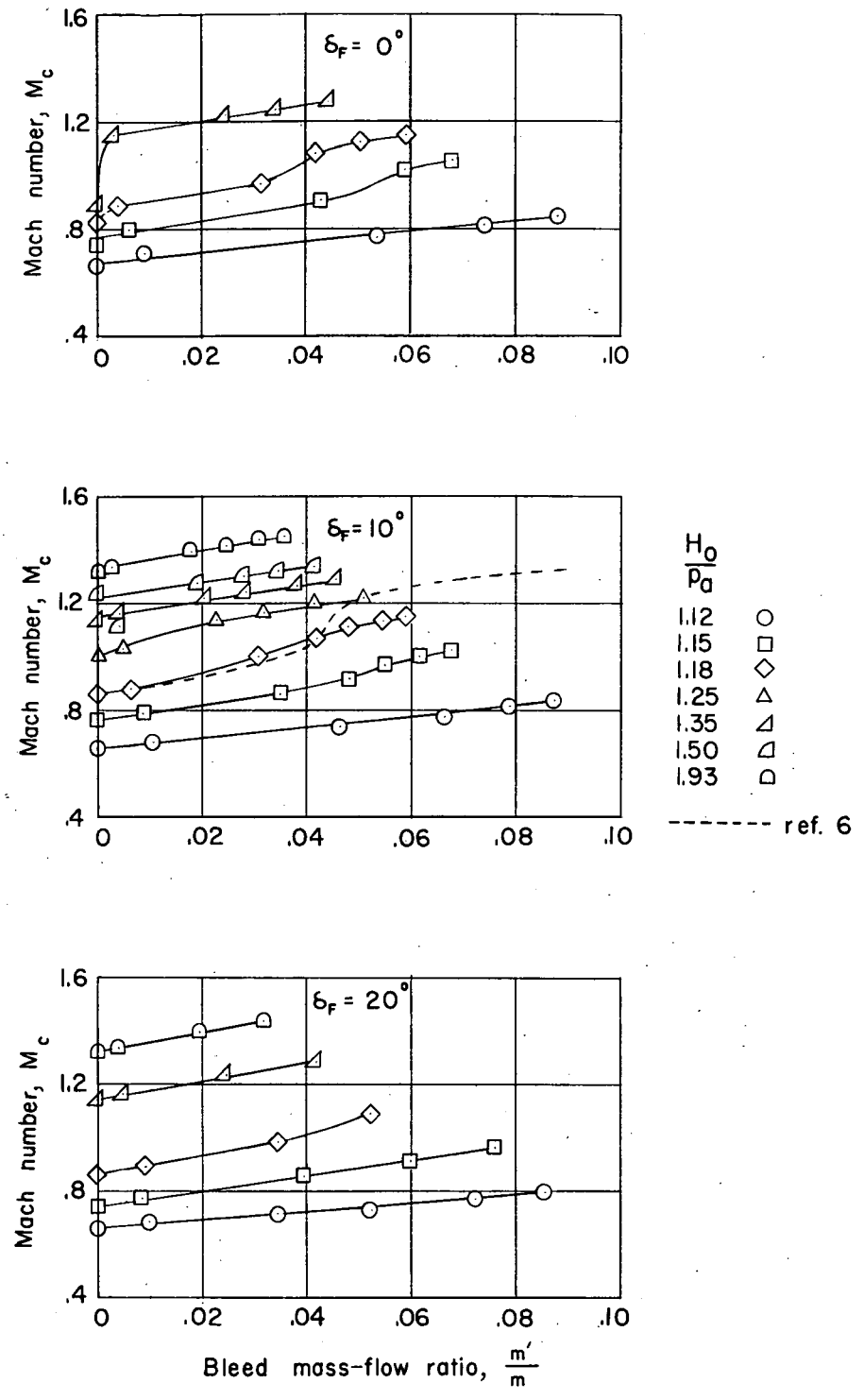

(a) Configuration II $\frac{y}{h/2} = .239$.

Figure 8. — Variation of test-section Mach number with bleed mass-flow ratio.

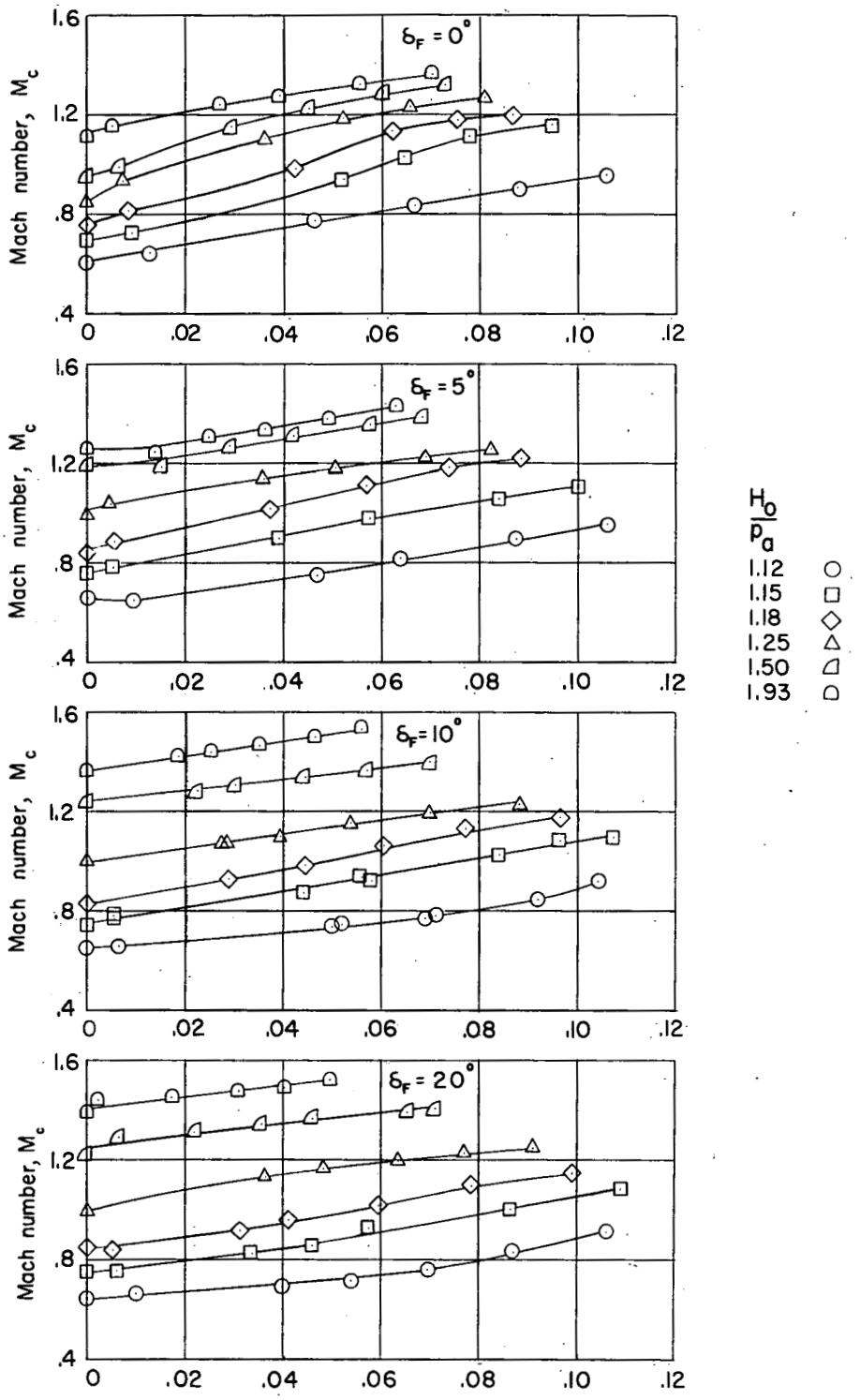

(b) Configuration III $\frac{y}{h/2} = .461$.

Figure 8.— Concluded.

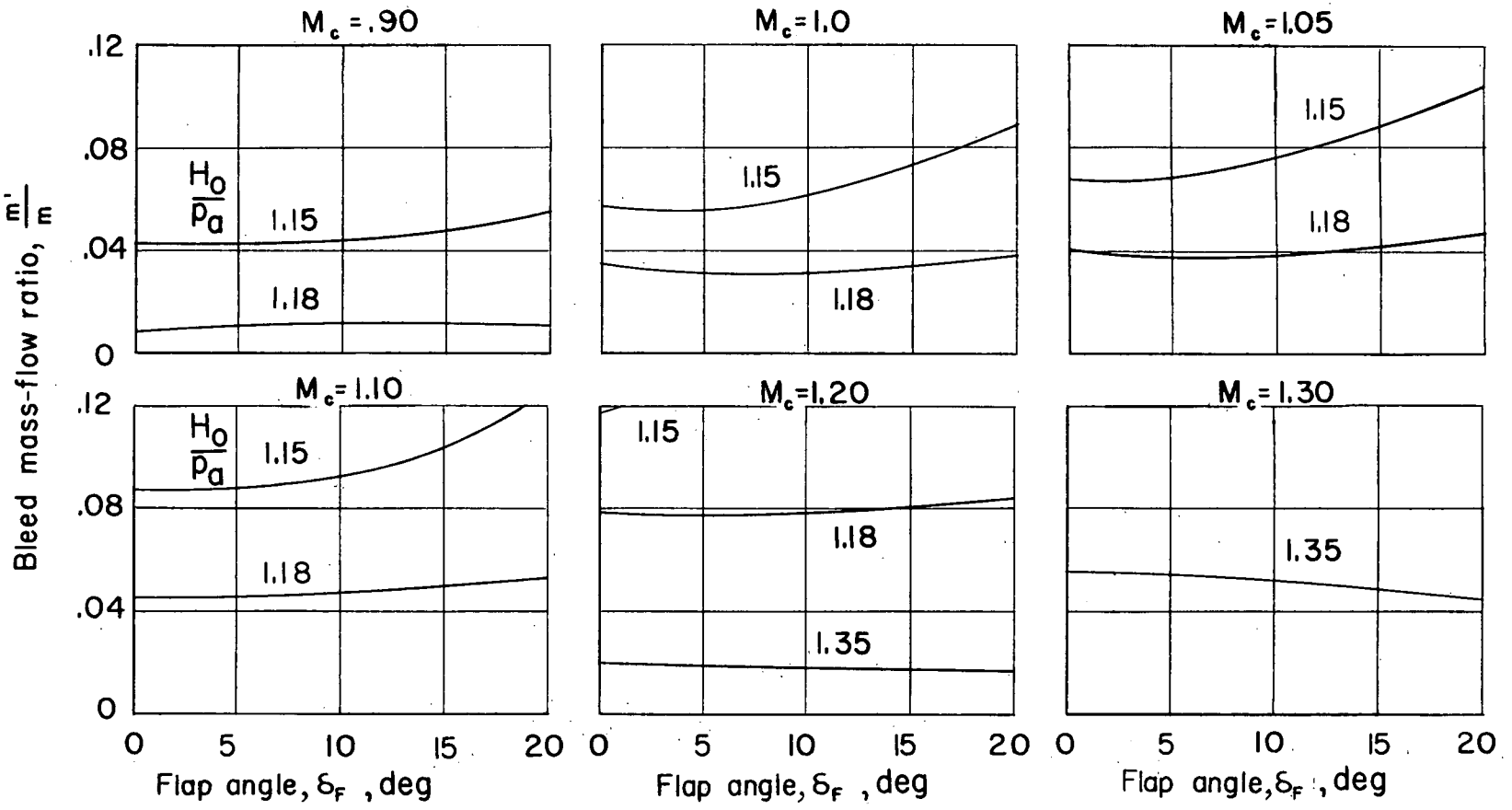

(a) Configuration II $\frac{y}{h/2} = .239$.

Figure 9. —Variation of bleed mass-flow ratio with flap angle for different Mach numbers.

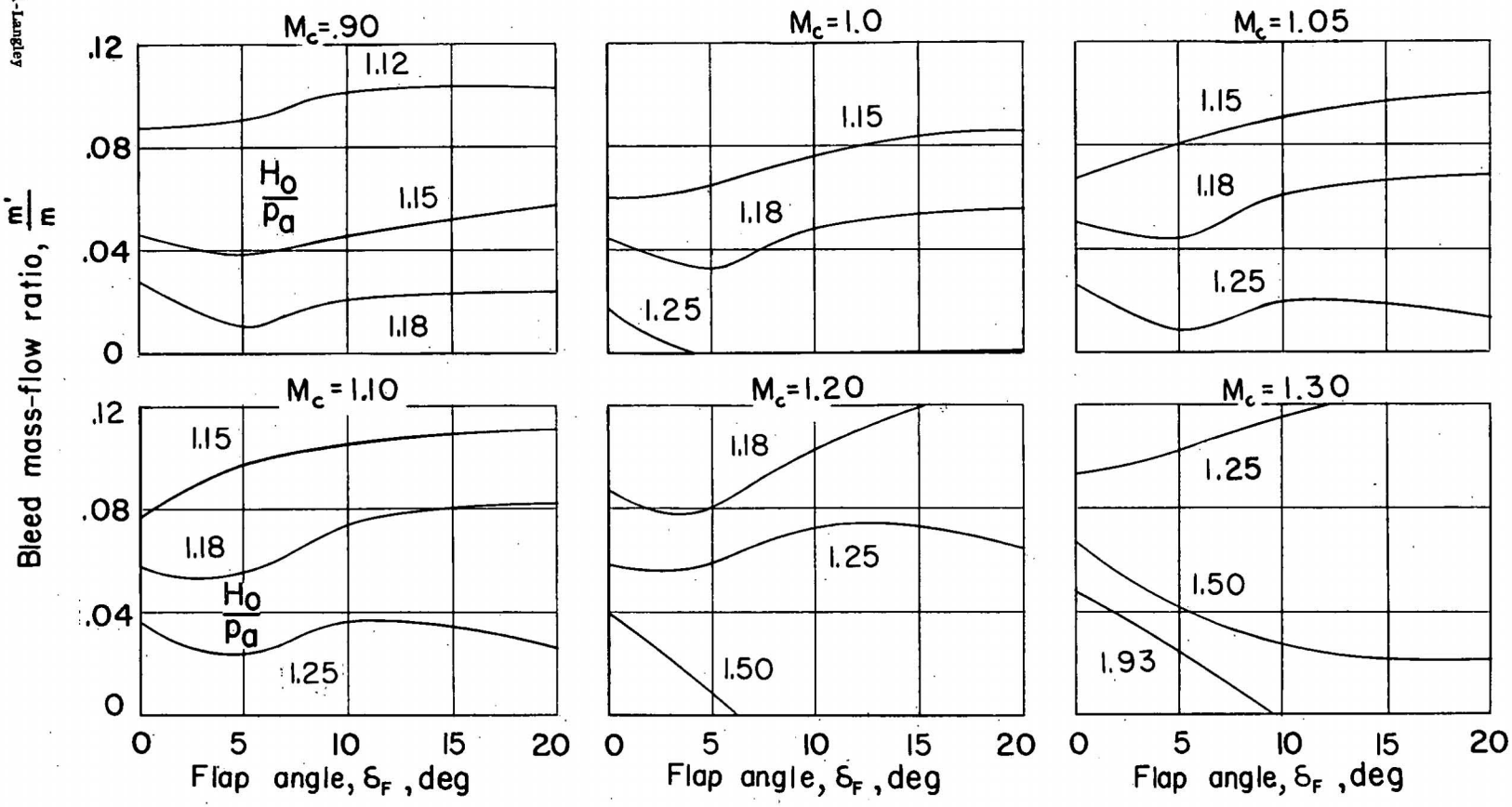

(b) Configuration III $\frac{y}{h/2}$ = .461.

Figure 9.— Concluded.